

# Study of Convective Temperature and Feedback Control

Tristan Schwab, Mitchell Braun, Ambrose Liu, Amy Jiang

*Department of Mechanical Engineering  
University of California at Berkeley*

## Abstract

The steady-state temperature of a cylindrical resistor is compared experimentally to a theoretical lumped capacitance model, and a PID controller is used to maintain a desired temperature by varying the supply voltage to the resistor-fan system. The purpose of this lab was to experimentally determine the temperature of a resistor measured using two temperature measurement systems at various supply voltages and study the relationship between convective flow supplied by a fan to the ambient temperature.

**Keywords**— Characterization, PID controller, lumped capacitance theory, temperature calibration

## Introduction

The control of temperature when it comes to electronics is crucial to various applications. Modeling a sophisticated control system is the best way to consistently keep the electronics at a safe and reliable temperature. In this lab the authors delve into the characterization of an experimental system for temperature control and implement a PID controller to control the experimental system. The experimental system is made up of a cooling structure with a fan mounted to the base producing forced-convection directed towards the top of the structure where a resistor is mounted. Topics explored in this lab aim to understand the relationship between theoretical heat transfer, control theory, uncertainty analysis, and data manipulation. The objective of this study is to develop a working controller that utilizes the theoretical model along with the system characteristics to build group understanding of implementing feedback control in industrial applications.

## Lab Theory

In this lab, the assumptions for a heated resistor encountering a uniform cross flow of air at a certain velocity are made. Figure 1. shows the resistor model for predicting the resistor temperature with different temperature conditions. The lumped capacitance

method (1) is used when assuming that the temperature across a body is uniform, with minimal internal conductive resistance and infinite thermal conductivity.

$$\frac{T - T_\infty}{T_i - T_\infty} = \exp\left(\frac{-hAt}{V\rho C}\right) \quad (1)$$

## Development of a Lumped Capacitance Model

### Question 1a

The lumped capacitance method assumes that the convection coefficient,  $h$ , is constant. To determine whether the lumped capacitance method is valid, use the general equation for the Biot Number, where  $L_c$  is the characteristic length for a cylinder ( $= \frac{r}{2}$ ).

$$Bi = \frac{hL_c}{K} = \frac{hr}{2K} \quad (2)$$

Lumped Capacitance is only applicable for Biot Numbers less than 0.1. Rearrange (2), holding  $r$  and  $K$  constant, the critical value for  $h$  must be less than  $0.2Kr$  or  $0.138 \frac{W}{m^2 K}$

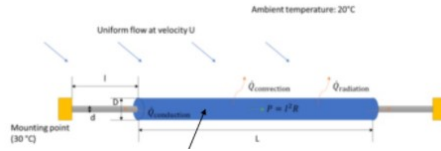


Figure 1: Cylindrical heated resistor in cross-flow

### Question 1b

The following form of the Lumped Capacitance method assuming no temperature time variance and using the resistors heat balance equation can be represented by the following case equation:

$$-\frac{V^2}{R} = k_l \frac{\pi d^2}{4l} (T_{ss} - T_m) + h(T_{ss} - T_\infty) \left( \frac{D_s}{2} l + 2\pi \frac{D_s^2}{4} \right) + \epsilon \sigma (T_{ss}^4 - T_\infty^4)$$

### Question 1c

If on the other hand, we assume that the conduction and radiation terms are negligible and there exists temperature and time variance, the general form of the lumped capacitance model becomes:

$$\rho V C_R \frac{dT}{dt} = -2\pi h (T_{ss} - T_{\infty}) \left( \frac{D_s}{2} h + 2\pi \frac{D_s^2}{4} \right) + \frac{V^2}{R}$$

### Question 1c

This equation can be integrated to a first order ODE which can be solved through an initial condition. The initial conditions can be determined from knowledge of the temperature at  $t = 0$ ,  $T_0$ .  $A$  is the surface area of the resistor exposed to the air. The assumptions made in this explicit derivation include convection is the only form of heat transfer, the temperature varies with time, with known initial temperature,  $T_0$ . The physical properties of air are constant and the ambient temperature is constant in space and time with a constant uniform cross sectional area throughout the ideal resistor.

$$\int_0^t \frac{dt}{\rho V C_R} = \int_0^T \frac{dT}{-2\pi h (T - T_{\infty}) A + \frac{V^2}{R}}$$

$$\theta = C_0 \exp\left[-\left(\frac{hA}{mC_R}\right)t\right] + \frac{V^2}{RhA}$$

### Question 2a

The heat transfer coefficient,  $h$ , of a heated cylinder can be found by rearranging the following relation for the Nusselt number:

$$Nu_D = \frac{hD}{k_R} \quad (3)$$

$$h = \frac{Nu_D K_R}{D} \quad (4)$$

For the case of **natural convection** in a horizontal isothermal cylinder, the Nusselt number and the corresponding  $h$  can be found by the following relation:

$$Nu_D = 0.36 + \frac{0.518 Ra_D^{1/4}}{[1 + (0.559/Pr)^{9/16}]^{4/9}} \quad (5)$$

where  $Ra_D$  represents the Rayleigh number,  $Pr$  represents the Prandtl number, and  $Re$  represents the Reynold's number.

$$Ra = \frac{g\beta(T_{ss} - T_{\infty})}{\alpha\nu} \quad (6)$$

$$Pr = \frac{\nu}{\alpha} \quad (7)$$

$$T(t) = T_{\infty} + \frac{V^2}{RhA} + (T_0 - T_{\infty} - \frac{V^2}{RhA}) \exp\left(\frac{-hAt}{mC_R}\right)$$

$$Re = \frac{U_{\infty}D}{\nu} \quad (8)$$

Where  $g$  is the acceleration due to gravity,  $\beta$ ,  $\alpha$ , and  $\nu$  are the fluid properties at the film temperature,  $T_s$  is the steady state temperature of the resistor, and  $T_{\infty}$  is the environment temperature while  $D$  is the outer diameter of the resistor.

### Question 2b

For **forced convection**, the following Nusselt correlation is applicable:

$$Nu_D = 0.3 + \frac{0.62Ra_D^{1/2}Pr^{1/3}}{[1 + (0.4/Pr)^{2/3}]^{1/4}} [1 + (\frac{Re}{282000})^{5/8}]^{4/5} \quad (9)$$

## PID Controllers

### Question 3

The PID controller is an instrument implemented in the current temperature control system by maintaining a nearly constant ambient temperature by adjusting power levels to the resistor and fan. An increase in temperature (above the critical temperature) would turn the fan on and vice versa with power to the thermistor. The way to examine the rise time, settling time, overshoot and the steady-state error is through an understanding of the parameters in the PID controller.

**P : Proportional tuning gain:** Corrects the target proportionally to the error difference. This component affects the rise time

**I : Integral tuning gain:** Cumulates the error associated with the proportional tuning gain and adjusts the temperature based on the cumulative error. This component drives the error to zero. This component affects the steady state error.

**D : Derivative tuning gain:** minimizes the overshoot from the integral tuning gain by slowing the correction factor applied. This component affects the overshoot error.

$$u(t) = K_p e(t) + K_i \int e(t) dt + K_d \frac{de}{dt} \quad (10)$$

## Study Methodology

### Procedure and Experimental Setup

In the first portion of the lab experiment, a theoretical model for the resistor temperature was developed to compare to actual data collected from the study. Characterization of the fan speed, resistor power, and resistor temperature were made. In the subsequent section, a working temperature PID controller was used to maintain the resistor temperature at a fixed measurement.

All measurements were performed on the National Instruments PXI system. After

opening LabView, the Type K thermocouple was connected to the NI DAQ block extension. 0, 4, 8, and 12 volts were supplied to the resistor with the fan turned off for twenty minutes to determine the steady-state resistor temperature. The steady-state temperature was then verified with the FLIR camera with a color map index.

After building the experimental relationship between steady-state temperature and supplied resistor voltage, the relationship between temperature and supplied voltage to the fan and resistor was recorded. A hotwire anemometer was used to measure the wind speed at various voltages to calibrate the fan voltage with respect to the wind speed.

Once the relationship between the fan, resistor, and temperature was developed, a Proportional-Integral-Derivative (PID) controller was initialized in Labview to maintain a consistent temperature of 25°C within a desired range by varying the supplied voltage to the fan. The resistor temperature was set to a sinusoidal function to simulate unwanted fluctuations. Temperature fluctuations were based on the gains applied in the PID controller (eq.6) which controlled the supplied voltage to the fan. A diagram illustrating the function of the PID controller is shown in figure 2. Note that the function of the PID controller can be referred to in the Theory section. Several combinations of gain parameters in the PID controller were tested until the desired parameters were identified to maintain the desired temperature within 5°C.

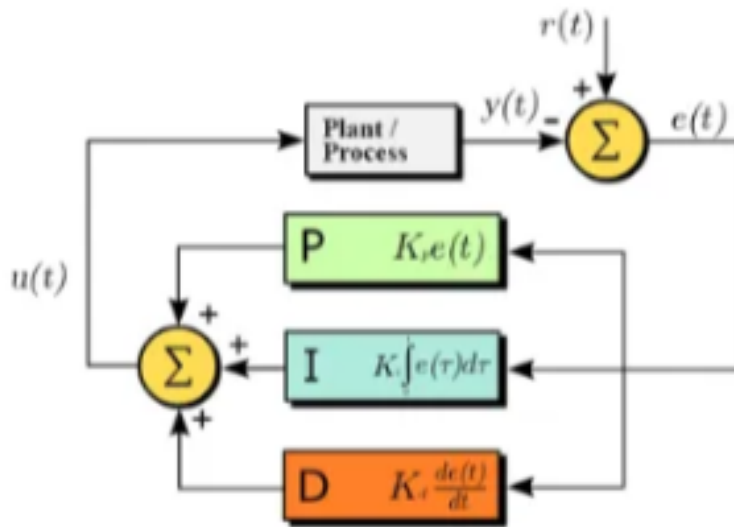


Figure 2: Block Diagram of the PID controller in a feedback loop

## Study Results and Discussion

### Question 4

The authors of this study used two techniques to measure the temperature, namely, taking measurements from a thermocouple and an FLIR (forward-looking infrared

camera). Figure 3 1 shows that the temperature measured by the thermocouple is lower than the measured temperature from the FLIR. This discrepancy arrives because thermocouple use a contact method to measure the surface temperature, but only measure at the point of contact due to heat conduction. Conversely, the FLIR camera will measure the thermal energy emitted by the body due to heat radiation. Due to the fact that the conductor is never a perfect blackbody, not all the thermal energy absorbed by the conductor will radiate out, only part of the thermal energy radiates out to the environment due to thermal radiation. As a result, the amount of thermal radiation received by the FLIR may not be as accurate as we expect.

Furthermore, we did not calibrate the FLIR camera. Without proper calibration, electronic component aging could lead to inaccurate temperature measurements. By using the default factory setup, whose accuracy is not guaranteed in the present experimental environment (this was noted by one of the authors that the default humidity was always set to zero percent and the ambient temperature was set to 22°C.)

Besides, the thermocouple is also susceptible to electromagnetic interference (EMI) due to noise in thermocouple signal. The IR camera can be affected by the surrounding environment. IR camera is mainly to receive radiation to reflect the temperature, but also to accept the radiation generated by the surrounding environment. Therefore, the receiver received not only the measured object radiation, and the final direct impact on temperature accuracy. From the experimental set-up, we also notice a temperature difference between the “shinier” surface and the brown-coated part of the resistor. Since the left “shinier” part is exposed to the heat source directly, the shinier surface radiate more heat than the brown-coated part. The brown-coated part also provides an extra thermal insulation layer to the resistor which block out the infrared radiation.

### Question 5b

Figure 5 shows a 3D surface plot comparison of the theoretical model and measured data. The main difference that is evident is that the model plot has a much higher temperature. This is to be expected, as the theoretical model ignores the effect of conduction and radiation (for the purposes of this study, convection was only taken into consideration). Therefore, the theoretical model, shown in red is overestimating the temperature while the measurement is lower due to real-world environmental factors such as radiation and heat conduction/dissipation.

### Question 5c

The range of wind speed and resistor power in which the model is valid compared to the measurement is from 4-9.2 m/s and 0-2.8 W, respectively. The resistor power is valid throughout both the measurement and model. The wind speed, as measured from the anemometer, is different for lower wind speeds (such as below 4 m/s). This is due once again to the fact that for the purposes of this study we considered only convection which makes the model overestimate the temperature, an affect which is more pronounced at low wind speeds.

## Question 6

The best gains used in this study for the PID controller to reach a desired temperature of 25°C. These gains were the following:

$$K_C = 5 \quad T_i = 3 \quad T_d = 2$$

The authors of this study found the best temperature control result with the associated PID gains based on [5] and adjusting values accordingly to reach a desired range of  $\pm 5^\circ\text{C}$ . Changing  $K_C$  increased the speed of the control response; however, the associated gain should not increase by too much or the process will begin to oscillate. The integral response would correct the error term over time, and the derivative response causes the output to decrease if the process output is increasing rapidly [5]. The PID gains are highly sensitive to noise, and given the noise in the system, too high of gains would make the system increasingly unstable.

## Contributions

Amy Jiang worked on Lab Theory question 2. Mitchell worked on Q5, Q6, and did the introduction. Ambrose worked on. Tristan worked on lab theory questions 1,2, and 3, lab methodology, and final report formatting in Latex.

## References

- [1] White, F. M., Fluid Mechanics, 4th ed. Blacklick, OH, USA: McGraw-Hill, 1998.
- [2] Sine fitting. (2020). MATLAB Central File Exchange. [Online] Accessed Oct. 10, 2020. Available: <https://www.mathworks.com/matlabcentral/fileexchange/66793-sine-fitting1>
- [3] Bergman, Fundamentals of Heat and Mass Transfer, 8th ed. Hoboken, NJ, USA: Wiley, 2017
- [4] Lienhard, A Heat Transfer Textbook, 5th ed. Cambridge, MA, USA: Some Phlogiston, 2020
- [5] "PID Theory Explained." NI, <https://www.ni.com/en-us/innovations/white-papers/06/pid-theory-explained.html#section-38687283>.
- [6] "Emissivity Affect on Thermal Imaging" FLIR, <https://www.flir.com/discover/professional-tools/how-does-emissivity-affect-thermal-imaging/> Accessed Mar. 10, 2022.

# 1 Appendix

|                      | $V_R = 0 \text{ V}$ | $V_R = 4 \text{ V}$ | $V_R = 8 \text{ V}$ | $V_R = 12 \text{ V}$ |
|----------------------|---------------------|---------------------|---------------------|----------------------|
| $V_F = 6 \text{ V}$  | 18.12               | 20.46               | 27.32               | 39.11                |
| $V_F = 12 \text{ V}$ | 17.82               | 19.21               | 24.12               | 32.32                |
| $V_F = 18 \text{ V}$ | 17.79               | 19.12               | 23.04               | 30.12                |

Table 1: Steady-state temperature ( $^{\circ}\text{C}$ ) with respect to fan and resistor voltage

| Fan Voltage | Wind Speed (m/s)   | Resistor Voltage | Temperature     |
|-------------|--------------------|------------------|-----------------|
| $V_F = 6$   | $U_{\infty} = 4$   | $V_R = 4$        | $T_{ss} = 32.2$ |
| $V_F = 12$  | $U_{\infty} = 6.9$ | $V_R = 8$        | $T_{ss} = 65.5$ |
| $V_F = 18$  | $U_{\infty} = 9.2$ | $V_R = 12$       | $T_{ss} = 110$  |

Table 2: Wind speed (m/s) measured using the hotwire anemometer at various voltages

Table 3: Steady-state resistor temperature ( $^{\circ}\text{C}$ ) measured by thermocouple with negligible convective flow

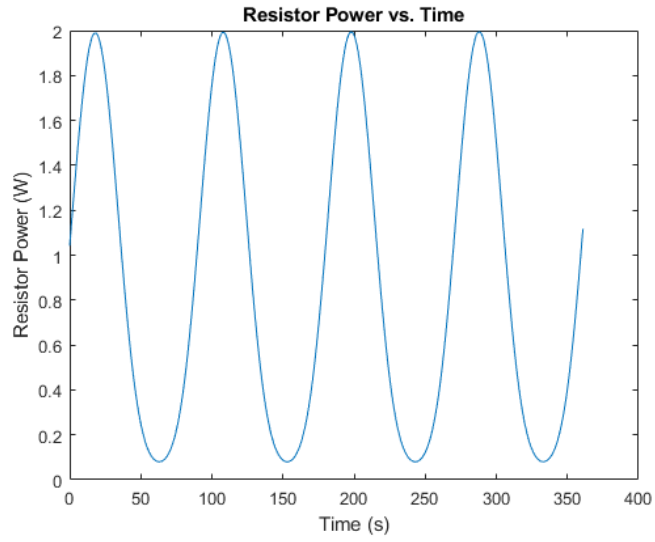


Figure 3: Power supplied to the resistor with respect to time

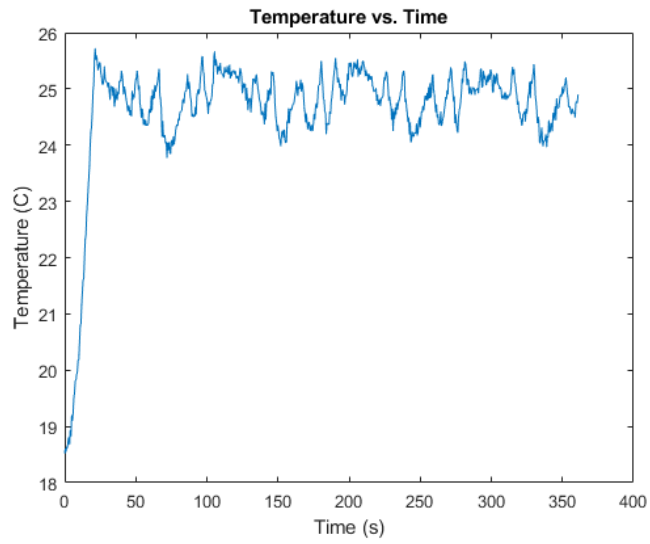


Figure 4: Temperature recorded with respect to time of the resistor

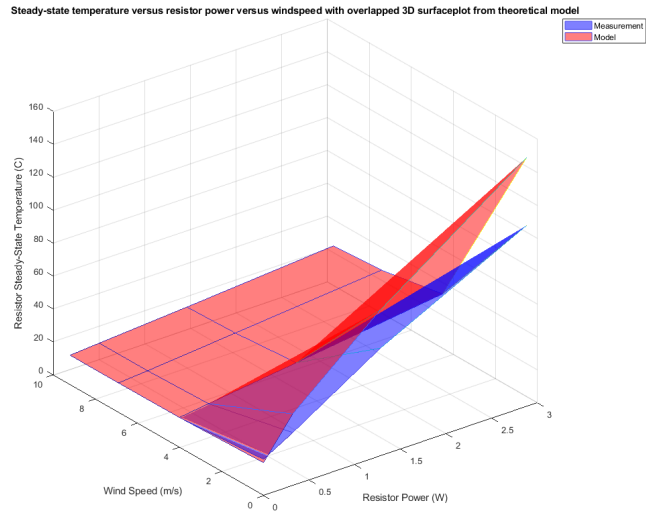


Figure 5: Steady-state temperature comparison with overlapped with theoretical model (Question 5a)

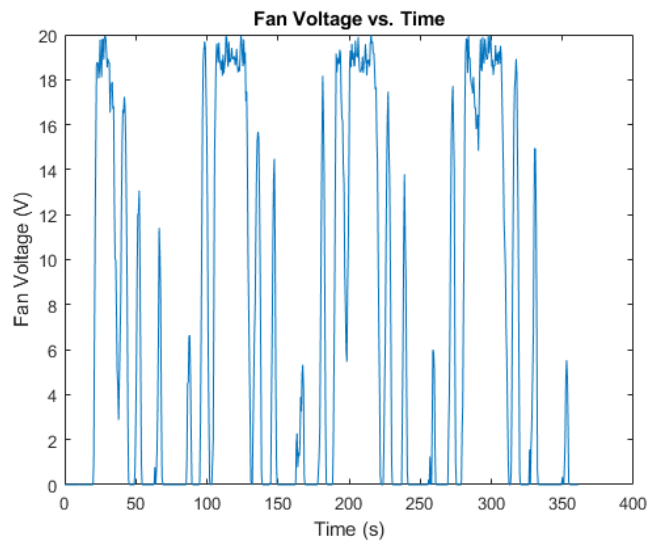


Figure 6: Fan voltage with respect to time

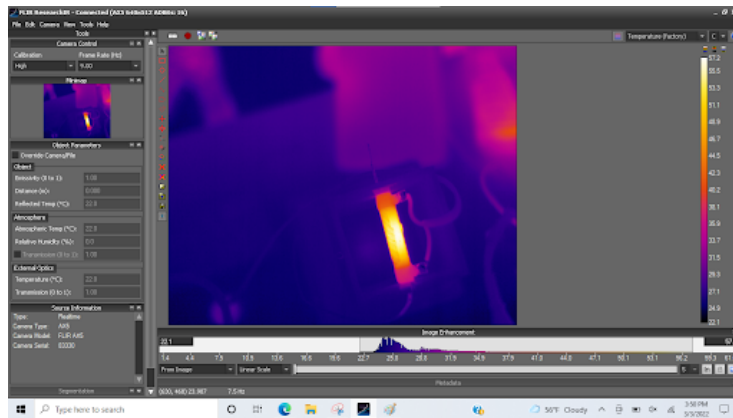


Figure 7: Temperature gradient of a resistor captured using the FLIR (forward-looking infrared camera)